Scale-Free Brain Functional Networks

Victor M. Eguíluz,[1] Dante R. Chialvo,[2] Guillermo A. Cecchi,[3] Marwan Baliki,[2] and A. Vania Apkarian[2]

[1]*Instituto Mediterráneo de Estudios Avanzados, IMEDEA (CSIC-UIB), E07122 Palma de Mallorca, Spain*

[2]*Department of Physiology, Northwestern University, Chicago, Illinois, 60611, USA*

[3]*IBM T.J. Watson Research Center, 1101 Kitchawan Rd., Yorktown Heights, New York 10598, USA*

(Received 13 January 2004; published 6 January 2005)

Functional magnetic resonance imaging is used to extract *functional networks* connecting correlated human brain sites. Analysis of the resulting networks in different tasks shows that (a) the distribution of functional connections, and the probability of finding a link versus distance are both scale-free, (b) the characteristic path length is small and comparable with those of equivalent random networks, and (c) the clustering coefficient is orders of magnitude larger than those of equivalent random networks. All these properties, typical of scale-free small-world networks, reflect important functional information about brain states.

DOI: 10.1103/PhysRevLett.94.018102 PACS numbers: 87.18.Sn, 87.19.La, 89.75.Da, 89.75.Hc

Recent work has shown that disparate systems can be described as complex networks, that is, assemblies of nodes and links with nontrivial topological properties, examples of which include technological, biological and social systems [1]. The brain is inherently a dynamic system, in which the traffic between regions, during behavior or even at rest, creates and reshapes continuously complex functional networks of correlated dynamics. An important goal in neuroscience is to understand these spatiotemporal patterns of brain activity. This Letter proposes a method to extract functional networks, as revealed by functional magnetic resonance imaging (FMRI) in humans, and analyze them in the context of the current understanding of complex networks (for reviews see [1–3]).

Figure 1 shows how underlying functional networks are exposed during any given task. In these experiments, at each time step (typically 400 spaced 2.5 sec.), magnetic resonance brain activity is measured in $36 \times 64 \times 64$ brain sites (so-called "voxels" of dimension $3 \times 3.475 \times 3.475$ mm^3). The activity of voxel x at time t is denoted as $V(x, t)$. We define that two voxels are *functionally connected* if their temporal correlation exceeds a positive predetermined value r_c, regardless of their *anatomical connectivity* [4,5]. Specifically, we calculate the linear correlation coefficient between any pair of voxels, x_1 and x_2, as

$$r(x_1, x_2) = \frac{\langle V(x_1, t)V(x_2, t)\rangle - \langle V(x_1, t)\rangle\langle V(x_2, t)\rangle}{\sigma(V(x_1))\sigma(V(x_2))}, \quad (1)$$

where $\sigma^2(V(x)) = \langle V(x, t)^2\rangle - \langle V(x, t)\rangle^2$, and $\langle\cdot\rangle$ represents temporal averages.

Figure 2 shows the degree distributions of networks extracted using this method. The data were collected while the subject was opposing fingers one and two during 10 sec, and then resting during 10 sec. We find a skewed distribution of links with a tail approaching a distribution $p(k) \sim k^{-\gamma}$, with γ around 2. This power law is more evident for networks constructed with higher thresholds r_c (more correlated conditions). For decreasing r_c, a maximum appears which shifts to the right. Despite changes in parameters, networks remain clearly defined indicating that the main conclusions are robust with respect to the selection of parameters. The small inset in Fig. 2 shows the distribution of links of a network constructed from the randomly shuffled (in time) voxels' signal. This network displays a Gaussian degree distribution in which the mean and width depend on r_c. The largest values of the correlation thresholds used to construct the random networks are usually extremely low ($r_c \sim 0.1$) compared to that used to

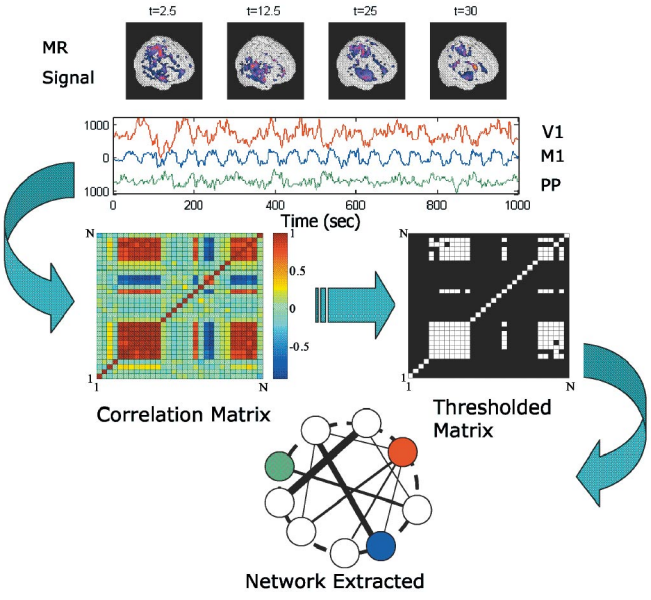

FIG. 1 (color). Methodology used to extract functional networks from the signals. The correlation matrix is calculated and then used to define the network among the highest correlated nodes. Top four images represent snapshots of activity and the three traces correspond to selected voxels from visual (V1), motor (M1) and posterio-parietal (PP) cortices.

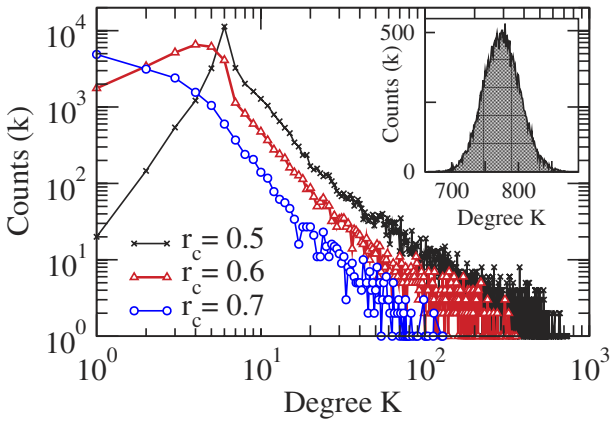

FIG. 2 (color online). Degree distribution for three values of the correlation threshold. The inset depicts the degree distribution for an equivalent randomly connected network.

define the functional networks ($r_c \sim 0.7$). Our data were also compared with values from a randomly rewired network, where nodes keep their degree by permuting links (i.e., the link connecting nodes i, $j$is permuted with that connecting nodes k, l) [6] (see below). In this control the degree of each node is maintained but all other correlations (including clustering) are destroyed.

To test the generality of these findings the same analysis was performed in seven subjects across three task conditions. During data acquisition [7] subjects perform on-off finger tapping with three different protocols. In one case they are instructed verbally to start and stop tapping, in the other one the start or stop cue is a small green or red dot in a video screen, and in the last one the start or stop cue is the entire screen turning green or red. The results are very robust across subjects and task conditions. In particular, the average of degree distribution (see Fig. 3) shows a clear power law scaling decaying as $p(k) \sim k^{-\gamma}$, with an exponent close to 2. Although a precise fitting is arguably difficult, we find that for $r_c = 0.6$ $\gamma = 2$, for $r_c = 0.7$ is 2.1, and for $r_c = 0.8$ is 2.2. This power law, indicating that the functional networks are scale-free, implies that there is always a small but finite number of brain sites having broad ''access'' to most other brain regions. Those well connected nodes are comparatively much more numerous in these networks than in a randomly connected network.

As shown in the bottom panel of Fig. 3 the average probability of finding a link between two nodes, separated at least by a distance Δ, also decays as a power law. The significance of the scaling with distance is unclear because of the well-known extensive cortex folding, which makes linear distance a dubious parameter.

The scale-free character remains unaltered even for tasks engaging different brain regions. This is already implicit in the aggregated data of Fig. 3 (top panel), but we further corroborated this feature by analyzing two radically different brain states: listening to music and

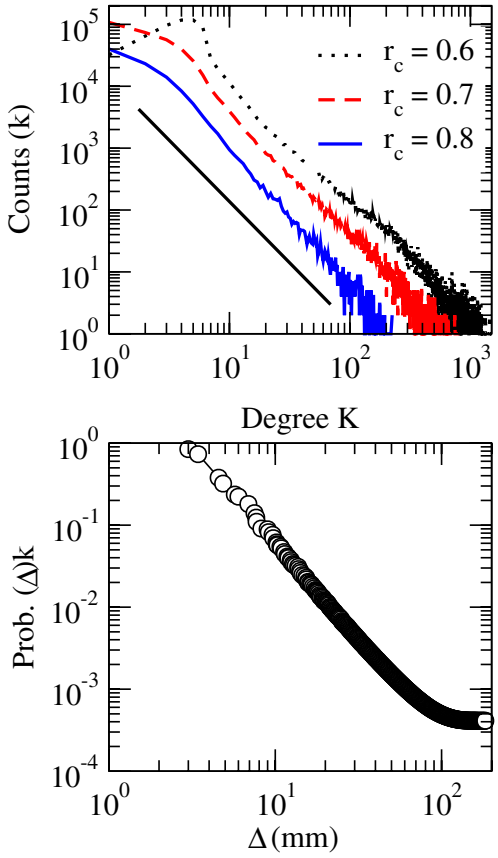

FIG. 3 (color online). Average scaling taken from 22 networks extracted from seven subjects. Top Panel: Average degree distribution. The straight line illustrates a decay of k^{-2}. Bottom panel: Average probability of finding a link between two nodes separated by a distance larger than Δ (using $r_c = 0.6$).

finger tapping. As shown in Fig. 4, although the topographic distribution of the functional networks is very different for the two tasks, they have similar scaling behavior. For comparison, the standard activation map derived with the generalized linear model [8] is also shown.

Now we turn to describe statistical properties of these networks: path length and clustering. The path length (L) between two voxels is the minimum number of links necessary to connect both voxels. Clustering (C) is the fraction of connections between the topological neighbors of a voxel with respect to the maximum possible. If voxel i has degree k_i, then the maximum number of links between the k_i neighbors is $k_i(k_i - 1)/2$. Thus, if E_i is the number of links connecting the neighbors then the clustering of voxel i, $C_i = 2E_i/k_i(k_i - 1)$. The average clustering of a network is given by $C = 1/N\sum_i C_i$, where N is the number of voxels. Clustering was analyzed also with respect to degree. The average clustering over voxels with the same degree $C(k) = 1/N_k \sum_{j=\{i|k_i=k\}} C_j$, where the sum runs over the N_k voxels with degree k.

Table I summarizes the results for the networks analyzed showing the average values ($n = 22$ datasets) for each

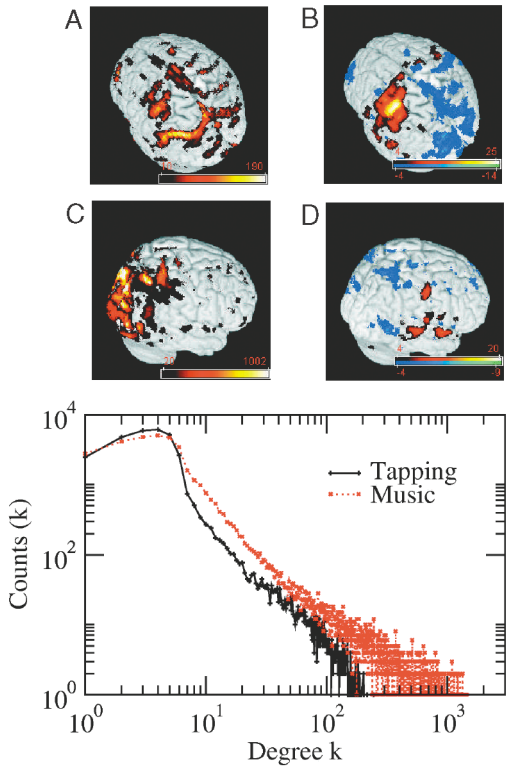

FIG. 4 (color). Comparison for two tasks: Panels (a) and (b) correspond to a finger tapping task while (c) and (d) to listening to music analyzed with our method or the standard FMRI linear model. Colors in pictures of panels (a) and (c) code the number of links detected with our method, and those in panels (b) and (d) the activation map built with standard model [8]. The link distributions (lower panel) show that the networks for both tasks are scale-free.

threshold (r_c, first column) used to construct the networks. Listed are N, C, L, the average degree $\langle k \rangle$, and γ. The clustering (C_{rand}) and path length (L_{rand}) values of an equivalent random network are also included for comparison. Note that as the threshold r_c increases the total number of nodes N decreases substantially, resulting by definition in more correlated networks. As a result, the number of nodes with at least one link decreases, and consequently the $\langle k \rangle$ value decreases as well. In all cases, the coefficient C remains 4 orders of magnitude larger than C_{rand}. Networks randomized using the rewiring described by Maslov et al. [6] also have clustering significantly smaller than the raw data (the order of 10^{-2}). This feature, together with the similarity of path length of the original nets and their randomized controls (L and L_{rand}), is indicative of a small-world structure [2,3]. This property is robust as it does not depend on parameter r_c.

To our knowledge, this is the first report on the topological structure of a large-scale brain network. Previous studies employing these statistical analyses have been limited to the small data sets of C. Elegans [2], and two neuroanatomical databases [9,10], the macaque visual cortex [11] and the cat cortex [12] (see Table II). These studies did not demonstrate scale-free features. Comparison with the previous two reports indicate the following: although clustering in the present study is smaller in absolute value, it is still orders of magnitude larger than the random case (10^{-1} vs 10^{-4}), while in the previous reports the clustering of the experimental data was just 1 order of magnitude larger than the randomized controls in the best case. Interestingly, the average connectivity $\langle k \rangle$ in all cases is of the same order, despite the huge differences in networks' origins and sizes. Accordingly, this consistency may reflect some constraint(s) inherent to network construction. These quantitative features show that the human brain network examined here has small-world properties, a finding that was previously postulated [2,3].

Figure 5 illustrates the dependence of two important features upon a voxel's degree. The first is clustering, found in many cases to scale as $C(k) \sim k^{-\alpha}$, an indication of hierarchical organization [13,14]. We see, instead, a relative independence of clustering from degree. The second feature is that a highly connected node tends to connect with other well connected nodes. As shown in the bottom panel of Fig. 5, there is a positive correlation between the degrees of adjacent vertices. This correlation, also called assortative mixing, is not typical of biological networks, but rather is distinctive of social networks [15]. Transitivity in correlations contributes to an artifactual increase of the clustering coefficient, using partial directed coherence or Granger causality [16] in the future should clarify this.

In summary, we report statistical measures showing that the functional correlations of the human brain form a scale-free network with small-world properties and assortative mixing. While some of these properties have been informally discussed, this work is the first quantitative description of these large-scale topological properties, as well as the first report of an assortative biological network. The scaling laws demonstrated here are robust across parame-

TABLE I. Average statistical properties of the brain functional networks.

r_c	N	C	L	$\langle k \rangle$	γ	C_{rand}	L_{rand}
0.6	31 503	0.14	11.4	13.41	2.0	4.3×10^{-4}	3.9
0.7	17 174	0.13	12.9	6.29	2.1	3.7×10^{-4}	5.3
0.8	4891	0.15	6.0	4.12	2.2	8.9×10^{-4}	6.0

TABLE II. Previously reported statistics of relatively smaller networks. None of these networks is scale-free.

Network	N	C	L	$\langle k \rangle$	γ	C_{rand}	L_{rand}
C. Elegans	282	0.28	2.65	7.68	not applicable	0.025	2.1
Macaque VC	32	0.55	1.77	9.85	not applicable	0.318	1.5
Cat Cortex	65	0.54	1.87	17.48	not applicable	0.273	1.4

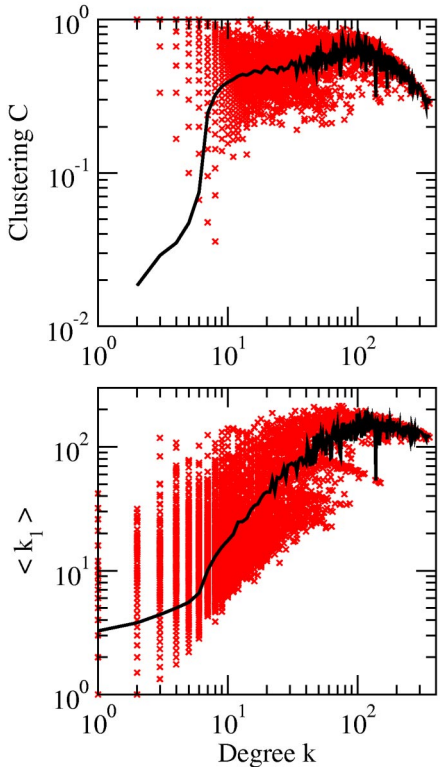

FIG. 5 (color online). Top Panel: Plot of clustering versus degree. Bottom panel: Plot of a neighboring node's degree versus degree illustrates the assortative feature. Symbols represents individual data and continuous lines the average values for nodes with the same degree. (Same subject shown in Fig. 2, with r_c=0.6).

ters (Fig. 1), subjects (Fig. 3), and task conditions (Fig. 4), suggesting they are invariant properties of an underlying dynamical network. The present results complement the extensive work done in the context of brain functional and effective connectivity [8,17]. The present approach has additional important implications. Namely, these studies can be extended to cases in which standard FMRI techniques cannot be used for lack of subject cooperation, (e.g., Alzheimer's patients). Because scale-free complex networks are known to show resistance to failure, facility of synchronization, and fast signal processing [18], it would be important to see whether brain networks' scaling properties are altered under various pathologies. In that regard, techniques for investigation of communities' structures [19] should be useful to analyze these aspects. Work on models [20] is needed to further clarify specific origins of the scaling laws. Overall, the network properties uncovered here offer a novel window to investigate the dynamics of brain states particularly in cases of dysfunction.

This work is supported by MCyT of Spain (Projects Nos. CONOCE2, BFM2002-12792-E, and FIS2004-05073-C04-03) and NIH NINDS of USA (Grants Nos. 42660 and 35115). D. R. C. is grateful for the hospitality and support of the Universitat de les Illes Balears, Mallorca, Spain.

[1] R. Albert and A.-L. Barabási, Rev. Mod. Phys. **74**, 47 (2002); M. E. J. Newman, SIAM Rev. **45**, 167 (2003).
[2] D. J. Watts and S. H. Strogatz, Nature (London) **393**, 440 (1998).
[3] S. H. Strogatz, Nature (London) **410**, 268 (2001).
[4] S. Dodel, J. M. Herrmann, and T. Geisel, Neurocomputing **44**, 1065 (2002).
[5] Networks can be defined using negative correlations; we restrict ourselves to the positive case only for simplicity.
[6] S. Maslov, K. Sneppen, and U. Alon, in *Handbook of Graphs and Networks*, edited by S. Bornholdt and H. G. Schuster, (Wiley-VCH and Co., Weinheim, 2003).
[7] Seven healthy, right-handed human subjects were studied using a Siemens-Trio 3.0 Tesla imaging system using a birdcage radio-frequency head coil. Blood oxygenation level-dependent single-shot echo-planar T2-weighted imaging was obtained using scan repeat time of 3000 ms, echo time of 30 ms, flip angle 90°, and field 256 mm. The data were preprocessed using the package FSL (http://www.fmrib.ox.ac.uk/fsl). All procedures employed were approved by Northwestern University Institutional Review Board.
[8] K. J. Friston, in *Brain Mapping: The Methods*, edited by A. Toga and J. Mazziotta, (Elsevier Science, New York, 2002).
[9] O. Sporns, G. Tononi, and G. M. Edelman, Cereb. Cortex **10**, 127, (2000); O. Sporns and G. Tononi, Complexity **7**, 28 (2003).
[10] C. C. Hilgetag, G. A. P. C. Burns, M. A. O'Neill, J. W. Scannell, and M. P. Young, Philos. Trans. R. Soc. London B **355**, 91 (2000).
[11] D. J. Felleman and D. C. Van Essen, Cereb. Cortex **1**, 1 (1991).
[12] J. W. Scannell, G. A. P. C. Burns, C. C. Hilgetag, M. A. O'Neil, and M. P. Young , Cereb. Cortex **9**, 277 (1999).
[13] E. Ravasz and A.-L. Barabási, Phys. Rev. E **67**, 026112 (2003).
[14] H. Jeong, S. P. Mason, A.-L. Barabási, and Z. N. Oltvai, Nature (London) **411**, 41 (2001).
[15] M. E. J. Newman, Phys. Rev. Lett. **89**, 208701 (2002).
[16] L. Baccala and K. Sameshima, Biol. Cybern. **84**, 463 (2001).
[17] B. Biswal, F. Z. Yetkin, V. M. Haughton, and J. S. Hyde, Magn. Reson. Med. **34**, 537 (1995).
[18] L. F. Lago-Fernandez, R. Huerta, F. Corbacho, and J. A. Siguenza. Phys. Rev. Lett. **84**, 2758 (2000).
[19] F. Radicchi, C. Castellano, F. Cecconi, V. Loreto, and D. Parisi, Proc. Natl. Acad. Sci. U.S.A. **101**, 2658 (2004).
[20] G. Caldarelli, A. Capocci, P. De Los Rios, and M. A. Muñoz, Phys. Rev. Lett. **89**, 258702 (2002).